energies

MDPI

Article

Experimental Investigation of the Heat Transfer Characteristics of Plate Heat Exchangers Using LiBr/Water as Working Fluid

Junhyeok Yong [1], Junggyun Ham [1], Ohkyung Kwon [2] and Honghyun Cho [3,*]

[1] Department of Mechanical Engineering, Graduate School of Chosun University, 309 Pilmundaero, Dong-gu, Gwangju 61452, Korea; yjh020800@naver.com (J.Y.); orchiders@chosun.kr (J.H.)
[2] Clean Energy R&D Department, Korea Institute of Industrial Technology, Cheonan-si 31056, Korea; kwonok@kitech.re.kr
[3] Department of Mechanical Engineering, Chosun University, 309 Pilmundaero, Dong-Gu, Gwangju 61452, Korea
* Correspondence: hhcho@chosun.ac.kr; Tel.: +82-62-230-7050; Fax: +82-62-230-7055

Abstract: In this study, the heat exchange characteristics of water–LiBr solutions used as working fluid in a plate heat exchanger (PHE) were experimentally investigated at various concentrations. To analyze the heat transfer characteristics under LiBr/water conditions, a brazing type plate heat exchanger was installed, and the LiBr concentration on the high-temperature side was controlled at 56%, 58%, 60% and 60%. The results showed that the average heat transfer rate under water/water conditions was higher than that under LiBr/water conditions and the average heat transfer rate decreased as the LiBr concentration on the hot side increased. In addition, under both water/water and LiBr/water conditions, the average heat transfer rate and overall heat transfer coefficient increased as the mass flow rate of the working fluid on the hot side increased. When LiBr was used, the Reynolds number (Re) of LiBr on the hot side was more than nine times lower than that of water at the same mass flow rate owing to the influence of the increased viscosity. Based on the data obtained from the water/water and LiBr/water experiments, a correlation for predicting the Nusselt number (Nu) on the hot side in a wide range was developed.

Keywords: heat transfer coefficient; pressure drop; plate heat exchanger; LiBr solution; concentration; Nusselt number (Nu)

Citation: Yong, J.; Ham, J.; Kwon, O.; Cho, H. Experimental Investigation of the Heat Transfer Characteristics of Plate Heat Exchangers Using LiBr/Water as Working Fluid. *Energies* **2021**, *14*, 6761. https://doi.org/10.3390/en14206761

Academic Editor: Andrzej Teodorczyk

Received: 3 October 2021
Accepted: 14 October 2021
Published: 17 October 2021

1. Introduction

With the rapid global industrial and economic growth in recent years, energy consumption has been increasing worldwide, leading to intensified global warming and environmental damage. Regulations on greenhouse gas emissions have accordingly been reinforced to mitigate global warming. Various problems with respect to refrigeration and cooling systems have been identified in light of their potential environmental impact. Research on refrigeration and cooling systems is therefore essential because they directly affect the ability to maintain a pleasant living environment as well as industrial manufacturing in modern society [1]. R-12 and R-22, which are freon-based refrigerants, have traditionally been used in refrigeration systems, while nowadays the use of natural refrigerants, such as R717 and R744, as well as low-global warming potential (GWP) alternative refrigerants such as R1234yf and R1234ze, is encouraged. However, the fourth generation refrigerants, such as R1234yf and R1234ze, are more expensive than second and third generation refrigerants. In addition, natural refrigerants also have critical limitations, such as their toxicity, combustibility, and operating pressure. Therefore, continuous research on various types of refrigeration systems with low GWP is required.

Among the various refrigeration systems, absorption refrigerators are efficient in terms of their energy saving capabilities. This is because they require a relatively small amount of additional power to provide refrigeration using the latent heat of vaporization of the

refrigerants, which are based on absorbents with low ozone depletion potential (ODP) and GWP and evaporate under low-pressure conditions [2]. As their operation is possible with a supply of relatively low-temperature thermal energy, various heat sources (city gas, LPG, waste heat, and exhaust gas) can be applied, and they are used on a large industrial scale in places with large amounts of waste heat [3]. However, absorption systems have a low coefficient of performance (COP) as compared with conventional compression refrigeration systems, and it is difficult to reduce their size [4]. To address these issues, the optimization and performance improvement of the primary components, such as the generator, absorber, and solution heat exchanger, are required.

Several studies have focused on improving the performance of the primary components of absorption refrigeration systems, and many of them were conducted on absorbers and generators that applied LiBr as an absorbent. The absorber has a direct impact on the system size and performance, and the performance improvement of the entire system can be attained by improving its performance. Hosseinnia et al. [5] analyzed the vapor absorption rate inside free-falling droplets with a diameter of 4.4 mm in an adiabatic absorber and found that the operating pressure of the absorber is an important variable for the amount of supercooling according to the operating temperature and concentration. Asfand et al. [6] examined the absorption rate according to the solution inflow rate by performing computational fluid dynamics (CFD) simulations. They found that the absorption rate increased 2.5 times as the inflow rate increased. In a previous study related to the generator, Hu et al. [7] analyzed the flow characteristics of LiBr according to the arc of the horizontal column using CFD to model the column inside a plate-type generator. The results revealed that a new plate-type falling film generator could secure uniform solution distribution and stable oil film flow.

In general, absorption systems are equipped with a solution heat exchanger for heat recovery to reduce the heating load of the generator. The solution heat exchanger provides the dilute solution with a preheating load by recovering the thermal energy of the heated concentrate. Shell-and-tube heat exchangers have been mainly used as solution heat exchangers; however, the application of plate heat exchangers (PHEs) with high heat transfer performance has also been prevalent. PHEs can induce turbulence at a low Reynolds number (Re) by stacking a large number of corrugated heat transfer plates to improve the convective heat transfer and thus exhibit higher efficiency as compared to the performance of shell-and-tube heat exchangers [8,9]. There have been several studies in this regard. First, Kan et al. [10] analyzed the characteristics of PHEs according to the water/water heat exchange and investigated the heat transfer characteristics of PHEs in which heat transfer plates with chevron angles of 30°/30°, 60°/60°, and 30°/60° were stacked during single-phase flow. They found that an increase in the chevron angle causes an increase in the Nusselt number (Nu) and proposed a Nu correlation factor that considers the chevron angle. Attalla et al. [11] analyzed the thermal performance of PHEs according to the surface roughness of heat transfer plates and found that the average heat transfer rate and pressure drop increased as the relative roughness of the heat transfer plates increased from 2.6×10^{-4} to 9.8×10^{-4}. In addition, many previous studies analyzed the heat transfer characteristics and pressure drop of PHEs under the water/water condition [12–15].

However, the heat transfer performance of PHEs significantly varies depending on the thermal properties of the working fluid used. Thus, separate experiments are required when LiBr is used as the working fluid. Vega et al. [16] analyzed the COP variation and coolant operating conditions in the absorption system utilizing the PHEs with high heat transfer performance as a generator, condenser, and recovery heat exchangers. They showed the possibility of improving the performance of the absorption cycle through the application of PHEs. Jeong et al. [17] conducted CFD analysis and verification experiments for brazed plate heat exchangers with chevron, oval, and circular embossing patterns to develop a high-temperature recovery solution heat exchanger. They reported that the oval embossing pattern has higher heat transfer performance and lower pressure drop than chevron and circular embossing patterns under the same geometric and thermal

conditions. Kim et al. [18] analyzed the heat transfer and pressure drop according to the chevron angles of 30°, 45°, and 63°, and found that the heat transfer performance increased alongside the increase in chevron angle. Kwon et al. [19] investigated the influence of various chevron angles (60°, 120°, and mixed type) of a solution heat exchanger on the heat transfer and pressure drop. Based on the experiment results obtained, they proposed a Nu and friction coefficient correlation according to the chevron angle. Song et al. [20] experimentally investigated the PHE performance under the operating conditions of the recovery solution heat exchanger of an absorption refrigerator. They demonstrated that the Nu correlation of the existing water-based PHEs is inappropriate for predicting Nu under the operating conditions of a triple effect absorption chiller and proposed a Nu correlation for such operating conditions. In addition, Song et al. [21] derived a Nu and friction coefficient correlation according to the high chevron angle (θ = 78.5°) and low chevron angle (θ = 55.7°) in PHEs and determined inconsistencies by applying the experimental conditions reported in previous studies.

The aforedescribed studies [10–15] were experimental studies on water/water in PHEs, and previous studies on LiBr/LiBr [17–21] mostly analyzed heat transfer characteristics and developed Nu correlations according to the experimental conditions. However, the water/LiBr condition of heat transfer characteristics analysis in the falling file type generator [22–24], which is a component of the absorption system, has been variously conducted, but studies related to water/LiBr in the simple plate heat exchanger (brazed type and gasket type plate heat exchanger) are insufficient. Because water has a higher heat transfer performance than LiBr, it can create a lower absorbent temperature through additional heat exchange with liquid LiBr present at the front end of the absorber in an absorption system, thereby improving the absorption performance in the absorber. Heat recovery for separate heating is also possible using such a device. To this end, in this study, the heat transfer characteristics and performance of a brazed plate heat exchanger were experimentally investigated under the LiBr/water condition for additional cooling inside an absorption system. In addition, the water/water experiment was performed to compare the performance, and a new Nu correlation that is related to LiBr/water heat transfer according to the mass flow rate was derived. The derived Nu correlation based on the LiBr/water experiment was compared with the Nu correlations presented in previous studies (LiBr/LiBr and water/water), and a correlation for predicting Nu under conditions with a wide range of concentration values, including both the water/water and LiBr/water experiment results, was newly derived.

2. Materials and Methods

2.1. Experimental Apparatus

Figure 1a,b show the schematic diagram of the experimental setup used in this study and an actual image. The experimental setup consists of: (1) a solution tank for storing and heating LiBr and water, (2) a condenser for maintaining the concentration of the solution, (3) test PHE, (4) recovery PHE, (5) cooling PHE, and (6) a constant-temperature bath for cooling loads. In the solution tank, two 7.5-kW heaters for the preheating and concentration control of the LiBr solution and a pressure gauge (UNIK 5000, DE Druck, Boston, MA, USA) for pressure measurement were installed. (7) Solution pump was installed at a distance of 1.5 m from the front of the test PHE (DIC285-19F, Dong Il Brazing, Bucheon, South korea) to transport fluids on the hot and cold sides, and bypass lines were constructed to reduce the pump load and control the flow rate. The flow rates of the working fluids on the hot and cold sides were adjusted by employing RPM control using inverters. Resistance temperature detectors (RTDs) and differential pressure gauges (Model 230, Setra Systems, Boston, MA, USA) were installed at the inlets and outlets on the hot and cold sides to measure the heat transfer rate and differential pressure of the test PHE. In addition, (8) a mass flow meter (ALT mass type U, OVAL Corporation, Tokyo, Japan) was installed at the inlets of the test PHE on the hot and cold sides to measure the mass flow rates of the working fluids that flow in the system. The fluid on the hot side cooled in the recovery

PHE is transported to the storage tank on the hot side for heating, and the fluid on the cold side heated in the recovery PHE is transported to the low-temperature storage tank after exchanging heat with the coolant supplied from the 3RT constant-temperature bath in the cooling PHE. To minimize heat loss to the outside during experiments, the heat exchangers, valves, solution tank, and piping were insulated with glass wool that has high insulation performance.

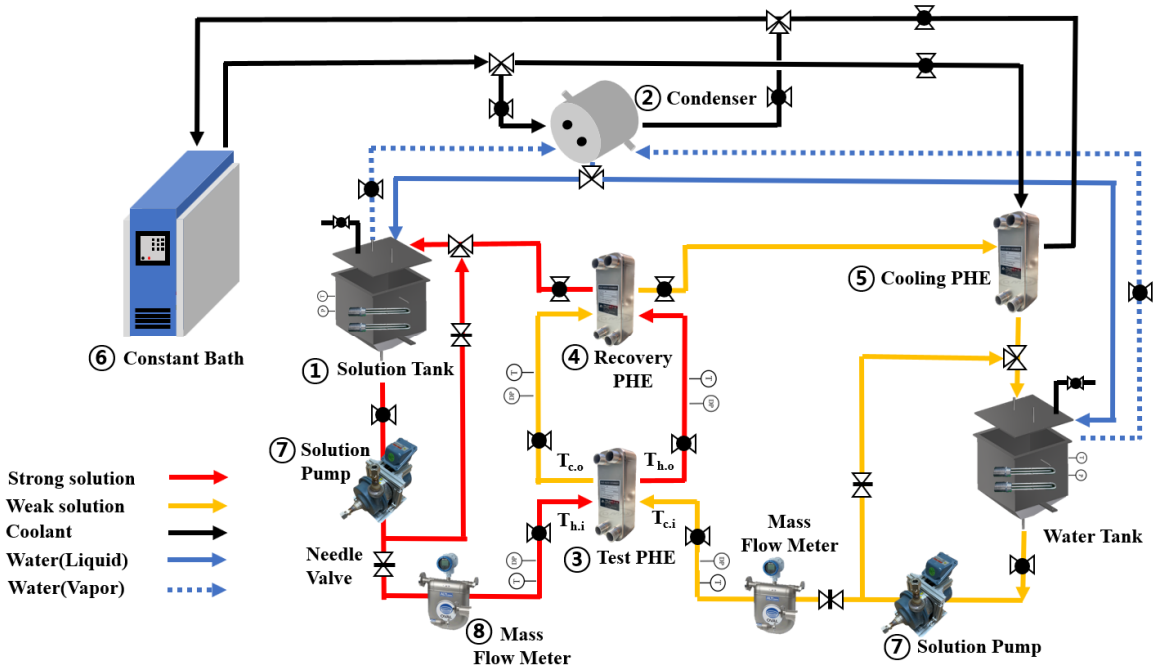

(**a**)

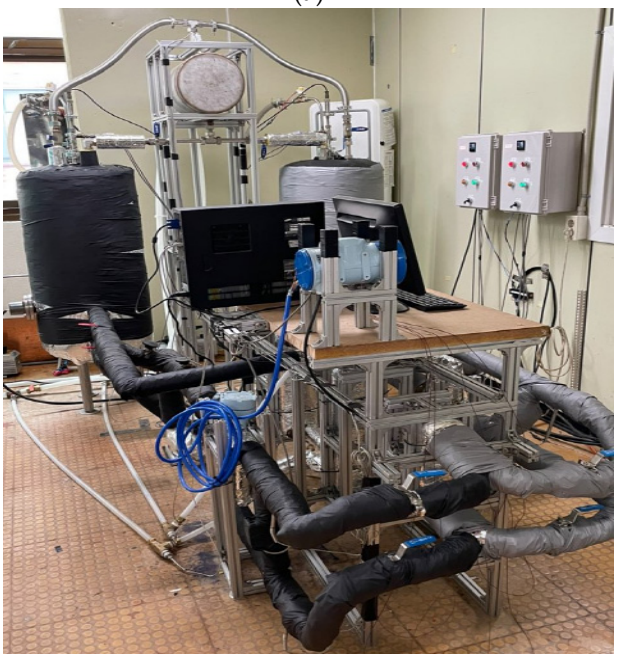

(**b**)

Figure 1. Schematic diagram and the image of experimental setup. (**a**) Schematic diagram of experimental setup: (1) Solution tank, (2) Condenser, (3) Test PHE, (4) Recovery PHE, (5) Cooling PHE, (6) Constant temperature bath, (7) Solution pump, and (8) Mass flow meter. (**b**) Image of experimental setup.

Figure 2 and Table 1 show the geometry and detailed geometrical information of the test PHE used in this study.

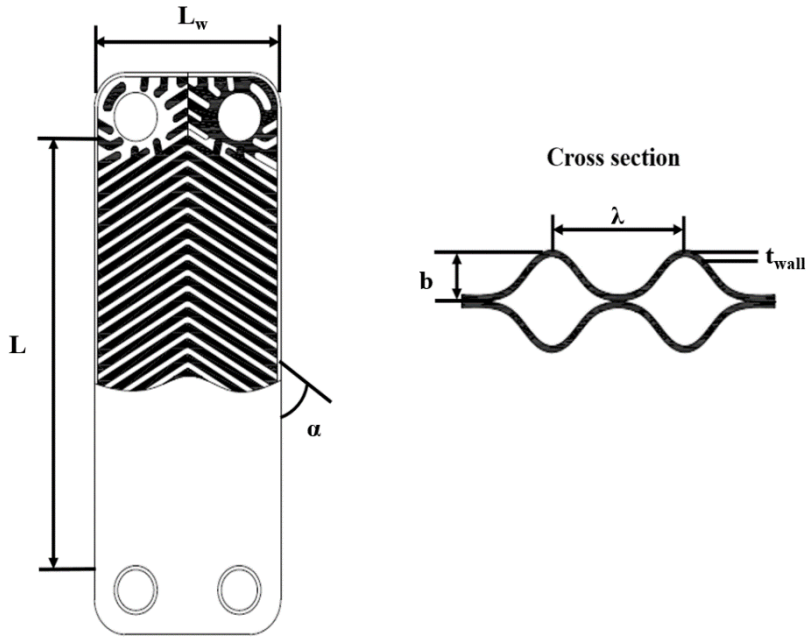

Figure 2. Schematic diagram of the test plate heat exchanger.

Table 1. Geometrical parameters of test plate heat exchanger.

Parameters	Dimension
Plate width, L_w	0.108 m
Plate length, L	0.203 m
Plate thickness, t_{wall}	0.0005 m
Corrugation depth, b	0.002 m
Corrugation pitch, λ	0.007 m
Chevron angle, α	60°
Number of plates, N	20
Number of channels, N_{ch}	9
Port diameter, D_{part}	0.025 m

The performance of the test PHE was measured under the steady-flow condition for 15 min, and the properties of LiBr for measuring the performance of the test PHE were calculated using Engineering Equation Solver (EES) based on the measured temperature and pressure.

Table 2 lists the experimental conditions used in the heat exchange experiment with water and LiBr. The inlet fluid temperatures on the cold and hot sides were fixed at 40 °C and 80 °C, respectively.

Water was used as a working fluid on the cold side. In this instance, the mass flow rate was fixed at 300 kg/h. Water and LiBr were used as a working fluid on the hot side, and the mass flow rate varied from 200 to 700 kg/h. When the working fluid on the hot side was LiBr, the concentration of LiBr was varied from 56% to 62%.

Table 2. Experimental conditions.

Type	Item	Cold Side	Hot Side
Water/water	Inlet fluid temperature, °C	40	80
	Mass flow rate, kg/h	300	200–700
	Reynolds number	250.4–289.7	210.9–832.1
LiBr/water	LiBr concentration, %	-	56, 58, 60, 62
	Inlet fluid temperature, °C	40	80
	Mass flow rate, kg/h	300	200–700
	Reynolds number	238–275.6	22.5–140.6

2.2. Data Reduction

2.2.1. Heat Transfer Analysis

The heat transfer rate of the test PHE is determined by the energy balance between the hot and cold sides, and in this study, it was calculated by the average $\left(\frac{Q_h+Q_c}{2}\right)$ of the heat transfer rates on the cold and hot sides. The heat transfer rates on the hot and cold sides can be expressed using Equations (1) and (2) as follows:

$$Q_h = \dot{m}_h c_{p.h}(T_{h,i} - T_{h,o}) \tag{1}$$

$$Q_c = \dot{m}_c c_{p.c}(T_{c,o} - T_{c,i}) \tag{2}$$

In addition, the overall heat transfer coefficient (U) in PHEs can be expressed by Equation (3). In this instance, the logarithmic mean temperature difference (ΔT_{LMTD}) that was used is given by Equation (4) [25]:

$$\mathrm{U} = \frac{Q_{avg}}{A_t \Delta T_{LMTD}} = \frac{1}{\frac{1}{h_h} + \frac{t_{wall}}{k_{wall}} + \frac{1}{h_c}} \tag{3}$$

$$\Delta T_{LMTD} = \frac{(T_{h,i} - T_{c,o}) - (T_{h,o} - T_{c,i})}{ln\left(\frac{T_{h,i} - T_{c,o}}{T_{h,o} - T_{c,i}}\right)} \tag{4}$$

where A_t is the effective heat exchange area of PHE ($\mathrm{A_t} = \varnothing \mathrm{L_w L N_{ch}}$), which is calculated using the heat transfer plate width (L_w), port-to-port distance (L), number of channels (N_{ch}), and expansion coefficient (ϕ). The expansion coefficient (ϕ) can be calculated using Equation (5) [26]:

$$\varnothing \approx \frac{1}{6}\left(1 + \sqrt{1 + \left(\frac{\pi b}{\lambda}\right)^2} + 4\sqrt{1 + \frac{1}{2}\left(\frac{\pi b}{\lambda}\right)^2}\right) \tag{5}$$

In general, Nu is defined by Equation (6) in single-phase flow. It is generally expressed as Equation (7) by empirical similarity:

$$Nu = \frac{hD_h}{k} = \frac{h}{k}\left(\frac{2b}{\varnothing}\right) \tag{6}$$

$$\mathrm{Nu} = \mathrm{A}Re^B Pr^C \tag{7}$$

where D_h is hydraulic diameter [21]. In this study, the Nu correlation was calculated using the Wilson plot method [27], and the constant C used in Equation (7) was fixed at 1/3 [28].

2.2.2. Uncertainty Analysis

Table 3 shows the detailed specifications of the measuring devices used in this study. Based on the measuring devices, the uncertainties of the thermal conductivity, convective heat transfer coefficient, and Nu be consistent using italics or not for this symbol obtained in the experiment were calculated. The experiment was performed at least three times under the same experimental conditions, and the average values were used to confirm the data. The general formula for the uncertainties of these values can be expressed as in Equation (8), and the uncertainties of the heat transfer rate, convective heat transfer coefficient, and Nu obtained in this study are shown in Table 4 [29]. In addition, the energy balance was investigated by calculating the heat gain and heat loss of the fluids on the hot and cold sides, which exchanged heat in the test PHE. When the energy balance on the hot and cold sides was examined under all conditions, the maximum error was found to be ±2.5%, indicating a relatively accurate energy transfer rate.

$$u_{exp} = \sqrt{\left(\frac{\Delta X}{X}\right)^2 + \left(\frac{\Delta Y}{Y}\right)^2 + \left(\frac{\Delta Z}{Z}\right)^2} \quad (8)$$

Table 3. Maximum uncertainties of measuring device.

Measurements	Model	Range	Accuracy
Temperature, °C	RTD PT100	−50–400	±0.5 °C
Mass flow rate, kg/h	ALT mass type U	0–1200	±0.1%
Pressure, kPa	UNIK 5000	0–20	±0.1%
Density, g/mL	ALT mass type U	0.32–2	±0.0005 g/mL

Table 4. Uncertainties of measurements.

Measurements	Uncertainty
Heat transfer rate	±2.4%
Heat transfer coefficient	±1.76%
Nusselt number	±3.37%

3. Results and Discussion

3.1. Comparison of Heat Transfer Performances of Water and LiBr

Figure 3 shows the heat transfer rate and heat transfer rate decrement ratio of LiBr/water compared to water/water according to the mass flow rate on the hot side. When the fluid on the hot side was water, the heat transfer rate increased from 7.56 to 12.13 kW as the mass flow rate increased from 200 to 700 kg/h. However, when the fluid on the hot side was a LiBr solution, the heat transfer rate decreased. In addition, the heat transfer rate decreased as the LiBr concentration increased, and the heat transfer rate was lowest when the concentration was 62%. At a mass flow rate of 200 kg/h, as the LiBr concentration increased from 56% to 62%, the heat transfer rate decreased from 4.19 to 3.8 kW, which is 44.5–49.6% lower compared with that of water. In contrast, at a mass flow rate of 700 kg/h, as the LiBr concentration increased from 56% to 62%, the heat transfer rate decreased from 9.49 to 8.88 kW, which were 21.7–26.8% lower compared with that of water. An increase in the mass flow rate of the working fluid increases the dependence on the heat transfer by the kinetic momentum of the fluid compared to the heat transfer that results from thermal diffusion during heat exchange by increasing the velocity of the fluid and the intensity of turbulence inside the PHE; thus, there is a decrease in the difference in heat transfer rate between water and LiBr.

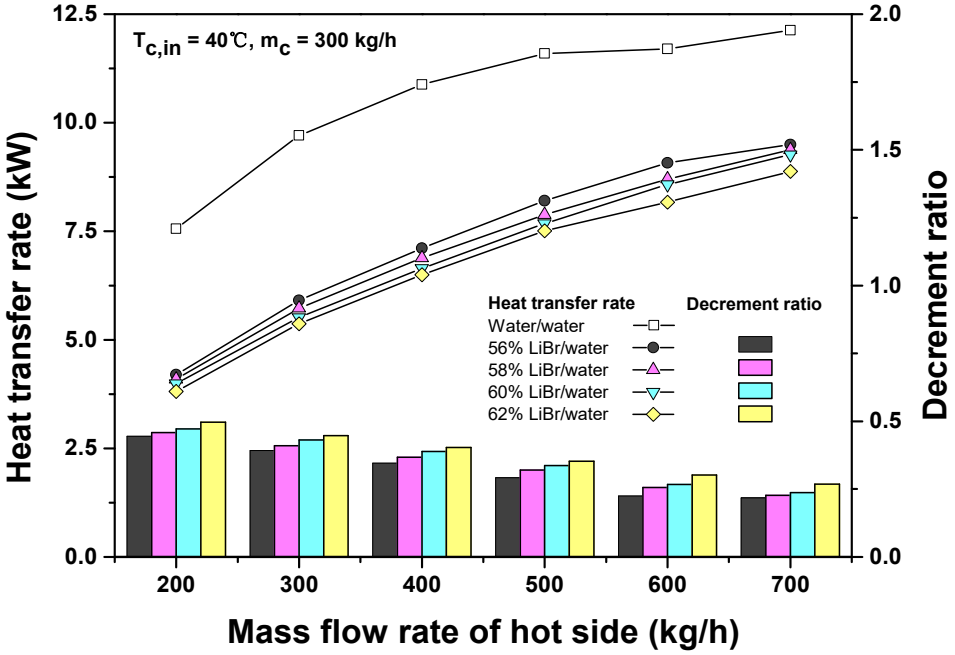

Figure 3. Variation in heat transfer rate and heat transfer rate ratio with the mass flow rate of the hot side.

Figure 4 shows the overall heat transfer coefficient and overall heat transfer coefficient decrement ratio of LiBr/water heat transfer compared to water/water according to the mass flow rate on the hot side in the water/water and LiBr/water experiments. When the working fluid on the hot side was water, the overall heat transfer coefficient increased from 1.38 to 2.03 kW/m^2·°C as the mass flow rate increased from 200 to 700 kg/h. When 56% LiBr was used as the working fluid on the hot side, the overall heat transfer coefficient increased from 0.76 to 1.43 kW/m^2·°C as the mass flow rate increased from 200 to 700 kg/h, which is 29.7% to 44.6% lower compared to water/water. When the highest concentration of 62% LiBr was used, the overall heat transfer coefficient increased from 0.637 to 1.177 kW/m^2·°C as the mass flow rate increased from 200 to 700 kg/h, which is 42.1–53.7% lower compared to water/water. The experiment results showed that the overall heat transfer coefficient decreased as the LiBr concentration increased. An increase in the LiBr concentration in PHEs results in a lower Re owing to the increase in the viscosity of the working fluid, and the reduced Re decreases convective heat transfer and makes thermal diffusion difficult, thereby reducing the overall heat transfer coefficient of LiBr compared to water.

3.2. Development of Nu Correlation

Figure 5 shows the Nu value of LiBr/water and water/water according to the mass flow rate on the hot side. In the water/water experiment, Nu increased from 13.91 to 33.39 as the mass flow rate increased from 200 to 700 kg/h. However, at 62% LiBr, which was the highest concentration in the LiBr/water heat exchange, Nu increased from 6.51 to 15.1 as the mass flow rate increased from 200 to 700 kg/h. In the LiBr/water heat exchange, an increase in LiBr concentration caused a decrease in Nu, resulting in values that were 46 to 60% lower compared to the Nu value of water/water at the same flow rate. In addition, when the lowest concentration of 56% LiBr was compared with the highest concentration of 62% LiBr, the difference in Nu between the two concentrations tended to slowly increase as the mass flow rate increased. This is because variations in thermal properties with concentration led to changes in the convective heat transfer performance by turbulence or diffusion even though it had the same heat transfer plate geometry.

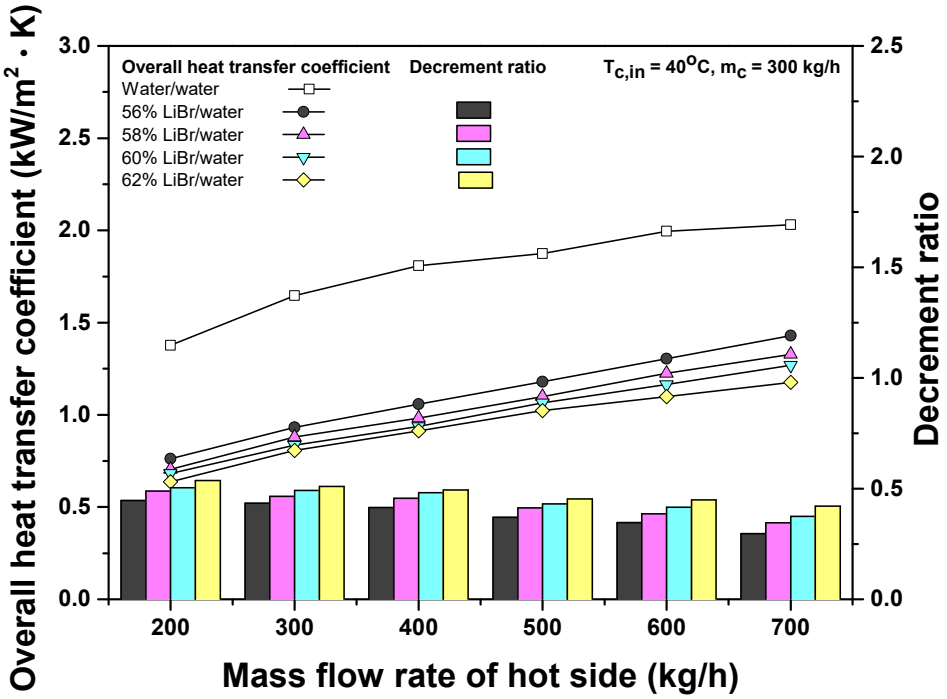

Figure 4. Variation in overall heat transfer coefficient and overall heat transfer coefficient ratio with mass flow rate of the hot side.

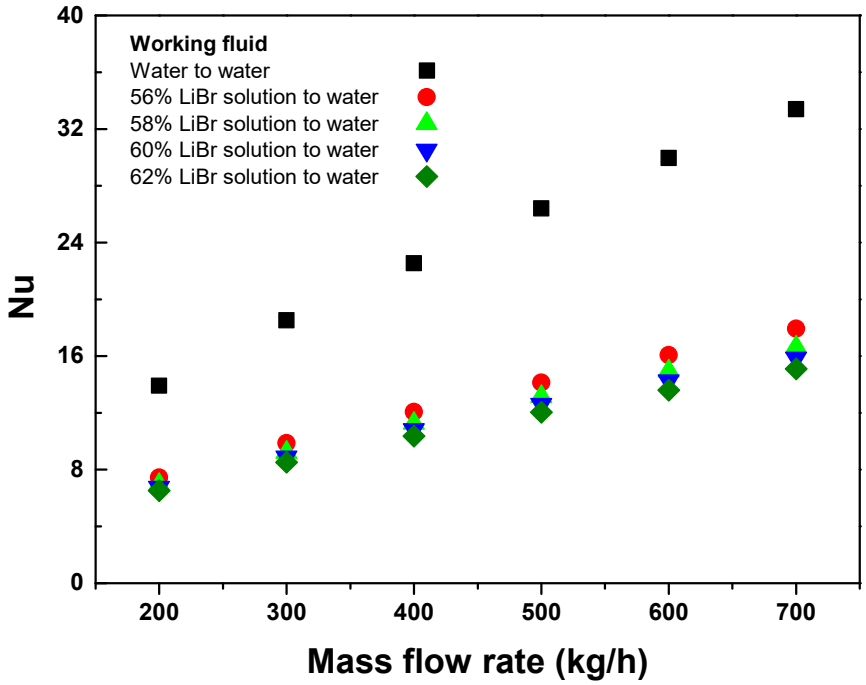

Figure 5. Variation in experimental Nu with mass flow rate of the hot side.

For PHEs, Nu varies depending on the geometry of heat transfer plates, flow conditions, and fluid characteristics. Various Nu correlations have been developed in previous studies. In this study, the suitability of the existing empirical formulas was determined by comparing the Nu correlations developed in previous LiBr/LiBr and water/water experiments with the results of the LiBr/water experiment. Figure 6 compares the Nu results obtained from the LiBr/water experiment with those derived from previous water/water experiments. In addition, the previous correlations used for the suitability of the experi-

ment results in this study are shown in Table 5. When the LiBr/water experimental values of this study were substituted into the Nu correlation developed by Roetzel et al. [30], Nu ranged from 8.97 to 24.79. These values were significantly higher compared to the Nu results based on the LiBr/water experiment in this study, which ranged from 6.51 to 17.93. The PHE used in Roetzel et al. [30] with a heat transfer plate length of 176.5 mm, a width of 71 mm, a heat transfer plate thickness of 0.5 mm, and a chevron height of 2 mm had similar geometry to the heat exchanger used in this study. However, the chevron angles were significantly different; 60° was used in this study and 20° was used in Roetzel et al. [30]. In general, the constant A in the empirical formula for Nu (Equation (7)) is determined by the heat transfer plate geometry. Therefore, there was a large difference in constant A between Roetzel et al. [30] (0.371) and the value in this study (0.28 to 0.324). In addition, when the LiBr/water experimental values were substituted into the Nu correlations presented in previous studies [30–33], all of the correlations predicted values that were higher than the Nu results in this study. In particular, the formula presented by Donowski and Kandlikar [31] predicted the highest value, and that presented by Focke et al. [32] exhibited the smallest error. Because the constants B and C in the empirical formula for Nu reflect the flow characteristics and thermal properties of the heat exchange medium, the difference in the value of each constant is caused by the difference in each experimental condition. As a result of comparing the Nu number correlation between the water/water in previous study and LiBr/water in this study, the B values of the Equation (7) were quite different. The B values of the LiBr/water condition in this study was 0.644–0.677, whereas the B values in previous studies [30–33] was 0.703 to 0.78. It was confirmed that the maximum difference of B value was 0.136. The shape of the plate heat exchanger used in previous studies was different from that in this study, but it was confirmed that the influence of thermal properties of the working fluid on the B value was relatively larger than the influence of shape of the plate heat exchanger. Therefore, when the Nu of LiBr/water was predicted through the correlations in previous studies developed through water/water experiments, the error rate exceeded 10%, confirming that there are limitations with respect to directly applying the correlations.

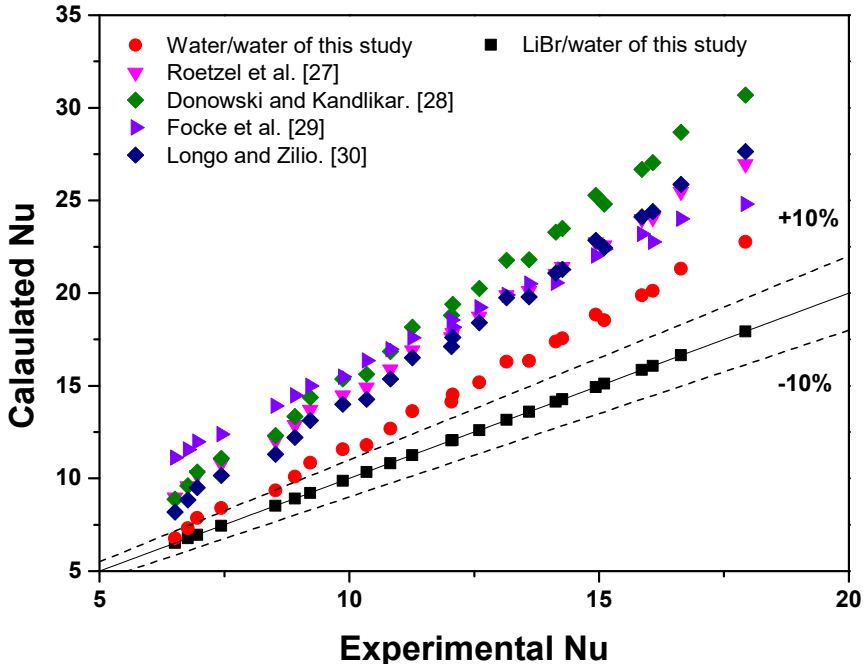

Figure 6. Comparisons of Nu of this study based on LiBr/water with existing Nu correlations of water/water.

Table 5. Previous correlations about Nu based on water/water $\left(\mathrm{Nu} = \mathrm{A}Re^{B}Pr^{C}\right)$

Reference	A	B	C	Comment
Roetzel et al. [30]	0.371	0.703	1/3	$400 < \mathrm{Pr} < 2000\ (\beta = 20°)$
Donowski and Kandlikar. [31]	0.2875	0.78	1/3	$10 < \mathrm{Pr} < 100\ (\beta = 60°)$
Focke et al. [32]	0.77	0.54	1/3	-
Longo and zilio. [33]	0.277	0.766	0.333	$200 < \mathrm{Pr} < 1200\ (\beta = 65°)$

Figure 7 compares the Nu results obtained from the LiBr/water experiment in this study with the prediction results of the Nu correlations presented in previous studies for LiBr/LiBr.

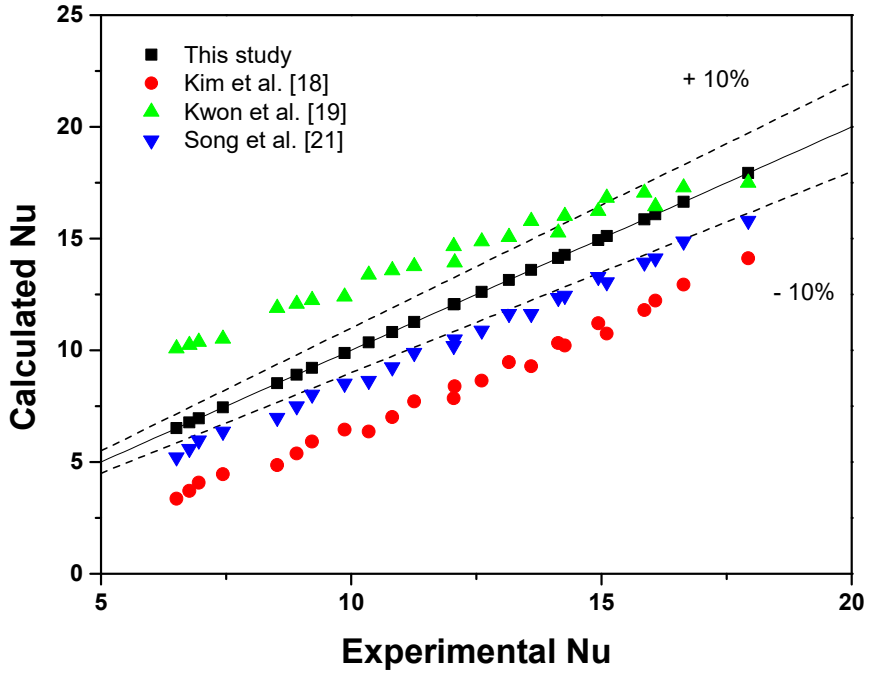

Figure 7. Comparison of Nu value for LiBr/water with existing correlation for LiBr/LiBr.

Tables 6 and 7 show the detailed geometrical information of PHE and experimental conditions in the previous studies. Because LiBr is generally used in absorption systems, it is difficult to make a direct comparison with the heat exchange results of LiBr/water. However, to the best of our knowledge, no extant study has investigated the difference, and it is therefore considered useful to examine the difference through this study. When the existing correlations based on LiBr/LiBr were compared with the LiBr/water results of this study, Kwon et al. [19] exhibited large errors of less than 60%, Song et al. [21] less than 30%, and Kim et al. [18] less than 50%. While Kim et al. [18] and Song et al. [21] showed tendencies similar to that of this study, despite the large errors in Nu, Kwon et al. [19] exhibited a significantly different increasing tendency for Nu compared to the results of this study. These differences occurred because experiments were performed at higher inlet temperatures in the previous studies compared to this study, and the previous studies had lower Nu results at similar Re levels as they had lower Prandtl numbers (Pr). In addition, Nu decreased because different geometrical parameters, such as the chevron angle, pitch, and height, cause a significant difference in the turbulence intensity of the secondary flow at the heat transfer plate contact point. As a result of comparing with Song et al. [21], there was no significant difference in the B values in Equation (7). The working fluid used in Song et al. [21] was LiBr/LiBr solution with a B value of 0.676. Also, the high-side working fluid under the LiBr/water condition in this study was a LiBr solution with B values of

0.644–0.677. In comparing B values, they were almost similar with a maximum difference of 0.03. On the other hand, since the shape of the plate heat exchanger used in this experiment and previous study [21] are different, the A values in Equation (7) were quite different. The A values in this study were ranged from 0.28 to 0.32, and that in the Song et al. [21] were 0.244, which indicating a relatively large difference with a maximum difference of 0.08. The B value was similar because the working fluid was the same as LiBr as hot-side working fluid, but the A value was differ due to the difference in the shape of the plate heat exchanger. A comprehensive analysis confirmed that it is somewhat difficult to predict the Nu of LiBr/water using the empirical formulas based on water/water [31–33] and LiBr/LiBr [18,19,21] presented in the previous studies. Therefore, it is necessary to develop a separate Nu correlation to identify Nu in the LiBr/water heat exchange process. In particular, the influence of geometry and working fluid must be accurately determined to predict the Nu of LiBr/water with high accuracy through the relatively easy water/water experiment. To this end, in this study, parameters A and B in the empirical formula for Nu were analyzed and functionalized according to variations in concentration by performing experiments. A and B are the empirical constants of $Nu = A\mathrm{Re}^{B}\mathrm{Pr}^{C}$ presented in Equation (7).

Table 6. Geometric parameters of plate heat exchanger in previous studies.

Reference	Chevron Angle, °	Plate Width, m	Plate Length, m	Corrugation Depth, m	Corrugation Pitch, m	Plate Number
Kim et al. [18]	30, 45, 63	0.192	0.519	0.0025	-	80
Kwon et al. [19]	120, 60, 60 × 120	0.119	0.289	0.002	0.006	20
Song et al. [21]	55.7, 78.5	0.111	0.4315	0.002	0.007	20
Present study	60	0.108	0.203	0.003	0.007	20

Table 7. Experimental condition in previous studies.

Reference	Item					
	x_h, %	x_c, %	m_h, kg/h	m_c, kg/h	T_h, °C	T_c, °C
Kim et al. [18]	62.5	53.2	5688–11,808	4140–11,088	125–160	80–95
Kwon et al. [19]	62.5	58.5	150–550	380	135–165	70
Song et al. [21]	50.21–64.92		181.8–1,063.8	75–154.7	26.24–125.6	
Present study	58–62	0	200–700	300 (Water)	80	40

Table 8 shows the results of A and B, which are the main parameters of the Nu correlation developed according to the LiBr concentration in LiBr/water heat exchange.

Table 8. Developed parameters of Nu correlation according to LiBr concentration in Equation (7).

LiBr Concentration, %	A	B	C
56	0.28	0.677	1/3
58	0.282	0.671	1/3
60	0.3	0.654	1/3
62	0.324	0.644	1/3

As the LiBr concentration on the hot side increased from 56% to 62%, parameter A increased from 0.28 to 0.324, but parameter B decreased from 0.677 to 0.644. In general, the mass flow rate of the working fluid and the concentration of LiBr are closely correlated to Re and Pr, which determine Nu. Because LiBr has a lower thermal diffusivity than water, the influence of the momentum of the fluid on convective heat transfer in PHE increases. Owing to the increasing influence of the PHE geometry, there is an increase in parameter A, which is directly related to the PHE geometry. In addition, when the

concentration of LiBr increases, the degree of increase in Re due to the increase in mass flow rate decreases. This is because the viscosity increases owing to the increase in LiBr concentration; therefore, parameter B decreases. In this study, parameters A and B are closely associated with the determination of Nu according to the LiBr concentration. Equation (9) shows the correlation for predicting Nu in LiBr/water heat exchange according to the LiBr concentration, which was developed in this study based on the water/water data. The developed correlation is applicable in the 221.1 < Re < 872.2 and 2.46 < Pr < 2.79 ranges under water/water condition:

$$Nu_{\text{pred}} = (\text{x}(1.067\text{x} - 0.1516) + 0.229)Re_w^{(0.69 - x(0.9x - 0.484))}Pr_w^{1/3} \quad (9)$$

Figure 8 depicts the error of the developed correlation compared to the experiment results obtained for LiBr/water. When the predicted Nu was compared with the experimental Nu, the error of 60% LiBr/water was 0.36% at a mass flow rate of 700 kg/h on the hot side, indicating high accuracy. At a flow rate of 200 kg/h, 58% LiBr/water exhibited the largest error of 2.15%. In addition, 58% LiBr/water showed the smallest error for Nu in the entire flow rate range, and 62% LiBr/water exhibited relatively large errors.

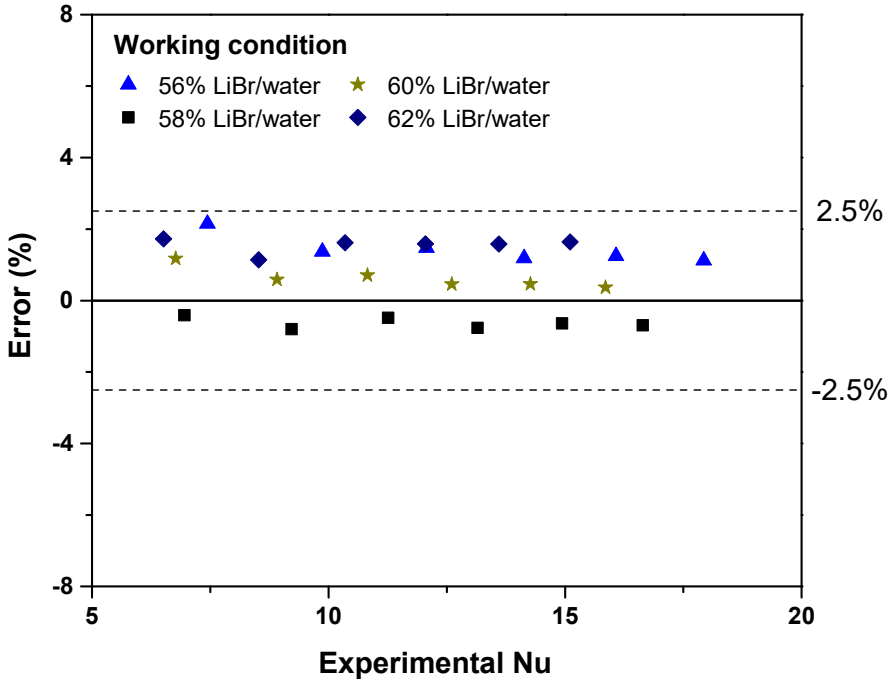

Figure 8. Deviation between predicted and experimental Nu.

4. Conclusions

In this study, the LiBr/water heat exchange characteristics in a plate heat exchanger (PHE) were experimentally analyzed, and a correlation for predicting the Nusselt number (Nu) during LiBr/water heat exchange was derived based on the water/water experiment results. The experimental results showed that the heat transfer rate and overall heat transfer coefficient decreased in LiBr/water heat exchange compared to water/water heat exchange, and they further decreased as the LiBr concentration increased. As the mass flow rate on the hot side increased from 200 to 700 kg/h, the heat transfer rate of water increased from 7.56 to 12.13 kW, but that of 62% LiBr increased from 3.8 to 8.88 kW, which were up to 26.8% lower compared to the case of using water. In addition, when the mass flow rate on the hot side increased from 200 to 700 kg/h, the overall heat transfer coefficient of water increased from 1.38 to 2.03 kW/m^2·°C, but that of 62% LiBr increased from 0.637 to 1.177 kW/m^2·°C, which were 42.1 to 53.7% lower compared to water.

When variations in Nu with LiBr concentration were examined and the average Nu decrement ratio was found to have increased to 7.19%, 12.12% and 17.32% as the LiBr concentration increased from 56% to 58%, 60%, and 62%, respectively. This is because changes in the properties of LiBr caused by the change in the LiBr concentration affected the heat transfer by heat transfer plate geometry, momentum, and thermal diffusion. In addition, a correlation for predicting Nu in LiBr/water heat exchange was developed (Equation (9)) based on the water/water heat transfer data. When the developed correlation was compared with the Nu results obtained through experiments, the error was found to be less than $\pm$2.5% under all conditions.

Author Contributions: Conceptualization, H.C. and J.H.; methodology O.K.; validation, O.K. and J.Y.; formal analysis, J.Y.; investigation, H.C. resources, J.H.; writing—original draft preparation, J.Y. and H.C.; writing—review and editing, H.C. and O.K.; supervision, H.C. All authors have read and agreed to the published version of the manuscript.

Funding: This work was supported by the Korea Institute of Energy Technology Evaluation and Planning (KETEP) and the Ministry of Trade, Industry & Energy (MOTIE) of the Republic of Korea (No.20202020800200).

Institutional Review Board Statement: Not applicable.

Informed Consent Statement: Not applicable.

Conflicts of Interest: The authors declare no conflict of interest. The funders had no role in the design of the study; in the collection, analyses, or interpretation of data; in the writing of the manuscript, or in the decision to publish the results.

References

1. Yamamoto, T.; Ozaki, A.; Lee, M. Optimal air conditioner placement using a simple thermal environment analysis method for continuous large spaces with predominant advection. *Energies* **2021**, *14*, 4663. [CrossRef]
2. Garc, Y.; Best, R.; Hugo, G.; Vargas, A.; Rivera, W.; Jim, C. A Cascade Proportional Integral Derivative Control for a Plate-Heat-Exchanger-Based Solar Absorption Cooling System. *Energies* **2021**, *14*, 4058.
3. Sun, J.; Fu, L.; Zhang, S. A review of working fluids of absorption cycles. *Renew. Sustain. Energy Rev.* **2012**, *16*, 1899–1906. [CrossRef]
4. Boruta, P.; Bujok, T.; Mika, Ł.; Sztekler, K. Adsorbents, Working Pairs and Coated Beds for Natural Refrigerants in Adsorption Chillers—State of the Art. *Energies* **2021**, *14*, 4707. [CrossRef]
5. Hosseinnia, S.M.; Naghashzadegan, M.; Kouhikamali, R. CFD simulation of adiabatic water vapor absorption in large drops of water-LiBr solution. *Appl. Therm. Eng.* **2016**, *102*, 17–29. [CrossRef]
6. Asfand, F.; Stiriba, Y.; Bourouis, M. CFD simulation to investigate heat and mass transfer processes in a membrane-based absorber for water-LiBr absorption cooling systems. *Energy* **2015**, *91*, 517–530. [CrossRef]
7. Hu, T.; Xie, X.; Jiang, Y. Numerical research on flow characteristics in a plate type falling film heat exchanger for a LiBr-H_2O absorption heat pump. *Procedia Eng.* **2017**, *205*, 485–491. [CrossRef]
8. Edreis, E.; Petrov, A. Types of heat exchangers in industry, their advantages and disadvantages, and the study of their parameters. *IOP Conf. Ser. Mater. Sci. Eng.* **2020**, *963*, 012027. [CrossRef]
9. Abou Elmaaty, T.M.; Kabeel, A.E.; Mahgoub, M. Corrugated plate heat exchanger review. *Renew. Sustain. Energy Rev.* **2017**, *70*, 852–860. [CrossRef]
10. Khan, T.S.; Khan, M.S.; Chyu, M.C.; Ayub, Z.H. Experimental investigation of single phase convective heat transfer coefficient in a corrugated plate heat exchanger for multiple plate configurations. *Appl. Therm. Eng.* **2010**, *30*, 1058–1065. [CrossRef]
11. Attalla, M.; Maghrabie, H.M. Investigation of effectiveness and pumping power of plate heat exchanger with rough surface. *Chem. Eng. Sci.* **2020**, *211*, 115277. [CrossRef]
12. Barzegarian, R.; Moraveji, M.K.; Aloueyan, A. Experimental investigation on heat transfer characteristics and pressure drop of BPHE (brazed plate heat exchanger) using TiO_2–water nanoflu. *Exp. Therm. Fluid Sci.* **2016**, *74*, 11–18. [CrossRef]
13. Saleh, B.; Sundar, L.S. Experimental study on heat transfer, friction factor, entropy and exergy efficiency analyses of a corrugated plate heat exchanger using Ni/water nanofluids. *Int. J. Therm. Sci.* **2021**, *165*, 106935. [CrossRef]
14. Huang, D.; Wu, Z.; Sunden, B. Pressure drop and convective heat transfer of Al_2O_3/water and MWCNT/water nanofluids in a chevron plate heat exchanger. *Int. J. Heat Mass Transf.* **2015**, *89*, 620–626. [CrossRef]
15. Behrangzade, A.; Heyhat, M.M. The effect of using nano-silver dispersed water based nanofluid as a passive method for energy efficiency enhancement in a plate heat exchanger. *Appl. Therm. Eng.* **2016**, *102*, 311–317. [CrossRef]
16. de Vega, M.; Almendros-Ibañez, J.A.; Ruiz, G. Performance of a LiBr-water absorption chiller operating with plate heat exchangers. *Energy Convers. Manag.* **2006**, *47*, 3393–3407. [CrossRef]

17. Jeong, J.Y.; Hong, H.K.; Kim, S.K.; Kang, Y.T. Impact of plate design on the performance of welded type plate heat exchangers for sorption cycles. *Int. J. Refrig.* **2009**, *32*, 705–711. [CrossRef]
18. Kim, H.J.; Kim, J.H.; Jeong, S.S.; Kang, Y.T. Heat transfer and pressure drop characteristics of plate heat exchanger for absorption application. *Proceedings SAREK Conference.* **2005**, 347–352.
19. Kwon, O.K.; Cha, D.A.; Yun, J.H.; Kim, H.S. Performance evaluation of plate heat exchanger with chevron angle variations. *Trans. Korean Soc. Mech. Eng. B* **2009**, *33*, 520–526. [CrossRef]
20. Song, J.Y.; Lee, J.W.; Kang, Y.T. Comparisons of Nu correlations for H_2O/LiBr solution in plate heat exchanger for triple effect absorption chiller application. *Energy* **2019**, *172*, 852–860. [CrossRef]
21. Song, J.Y.; Park, J.H.; Kang, Y.T. Heat transfer and frictional pressure drop characteristics of H_2O/LiBr solution in plate heat exchangers for triple-effect absorption application. *Appl. Therm. Eng.* **2021**, *189*, 116730. [CrossRef]
22. Ulcerations, P.F. Heat exchanger development for compact water/LiBr sorption systems 200 DRAFT Proceedings of IMECE2006. In Proceedings of the 6 ASME International Mechanical Engineering Congress and Exposition, Chicago, IL, USA, 5–10 November 2006; pp. 1–7.
23. Jeong, S.; Garimella, S. Falling-film and droplet mode heat and mass transfer in a horizontal tube LiBr/water absorber. *Int. J. Heat Mass Transf.* **2002**, *45*, 1445–1458. [CrossRef]
24. Killion, J.D.; Garimella, S. A review of experimental investigations of absorption of water vapor in liquid films falling over horizontal tubes. *HVAC R Res.* **2003**, *9*, 111–136. [CrossRef]
25. Chan, J.J.; Best, R.; Cerezo, J.; Barrera, M.A.; Lezama, F.R. Experimental study of a bubble mode absorption with an inner vapor distributor in a plate heat exchanger-type absorber with NH_3-$LiNO_3$. *Energies* **2018**, *11*, 2137. [CrossRef]
26. Zhu, X.; Haglind, F. Relationship between inclination angle and friction factor of chevron-type plate heat exchangers. *Int. J. Heat Mass Transf.* **2020**, *162*, 120370. [CrossRef]
27. Fernández-Seara, J.; Uhía, F.J.; Sieres, J.; Campo, A. A general review of the Wilson plot method and its modifications to determine convection coefficients in heat exchange devices. *Appl. Therm. Eng.* **2007**, *27*, 2745–2757. [CrossRef]
28. Alzahran, S.; Islam, M.; Saha, S. A thermo-hydraulic characteristics investigation in corrugated plate heat exchanger. *Energy Procedia* **2019**, *160*, 597–605. [CrossRef]
29. Zheng, D.; Wang, J.; Chen, Z.; Baleta, J.; Sundén, B. Performance analysis of a plate heat exchanger using various nanofluids. *Int. J. Heat Mass Transf.* **2020**, *158*, 119993. [CrossRef]
30. Roetzel, W.; Das, S.K.; Luo, X. Measurement of the heat transfer coefficient in plate heat exchangers using a temperature oscillation technique. *Int. J. Heat Mass Transf.* **1994**, *37*, 325–331. [CrossRef]
31. Djordjević, E.; Kabelac, S.; Šerbanović, S. Heat transfer coefficient and pressure drop during refrigerant R-134a condensation in a plate heat exchanger. *Chem. Pap.* **2008**, *62*, 78–85. [CrossRef]
32. Focke, W.W.; Zachariades, J.; Olivier, I. The effect of the corrugation inclination angle on the thermohydraulic performance of plate heat exchangers. *Int. J. Heat Mass Transf.* **1985**, *28*, 1469–1479. [CrossRef]
33. Longo, G.A.; Zilio, C. Condensation of the low GWP refrigerant HFC1234yf inside a brazed plate heat exchanger. *Int. J. Refrig.* **2013**, *36*, 612–621. [CrossRef]